Analysis of vortex merge graphs

Jens Kasten[1,2], Andre Zoufahl[1], Hans-Christian Hege[1], and Ingrid Hotz[1]

[1]Zuse Institute Berlin, Germany
[2]University of Leipzig, Germany

Abstract

We propose an analysis framework to investigate different flow quantities such as vorticity, λ_2 or the acceleration magnitude along vortex merge graphs and within their regions of influence. The explicit extraction of vortex merge graphs enables the application of statistical tools to investigate the vortex core lines themselves. The analysis tool provides common plots as scatter plots and parallel coordinates to explore the correlation of different quantities. An abstract representation of the vortex merge graph highlights birth, death and merges of vortices. Interactive picking of substructures supports a closer inespection of single vortices and their evolution. A further step integrates the regions of influence into the statistical analysis. Minima, maxima, median, mean and other percentiles of the measures along the vortex merge graph and its regions are visualized. The usability of the framework is demonstrated using a simulated flow data set of a mixing layer and a jet.

Categories and Subject Descriptors (according to ACM CCS): I.3.8 [Computing Methodologies]: Computer Graphics—Applications J.2 [Computer Applications]: Physical Sciences and Engineering—Physics

1. Introduction

The definition and extraction of vortices in fluid flows is topic of many discussions in the fields of fluid mechanics and flow visualization. Despite the importance of flow structures, there is still no unique mathematical definition of a vortex. Rather, the different kinds of applications entail different needs for appropriate vortex definitions. Recently, Kasten et al. proposed a method to explicitly extract vortex merge graphs in two-dimensional time-dependent data sets [KHNH12]. These graphs can be based on different quantities that identify vortices as extremal structures. In this paper we present an approach to evaluate and compare different vortex definitions. The goal is to support a better understanding of their differences and similarities. The analysis is driven by questions concerning the explicit time of merge events, the granularity of the resulting structures and the conservation of certain quantities transported by the vortices. Central to this analysis is an explicit vortex merge skeleton given as a graph embedded in three-dimensional space time. Together with an abstract representation this facilitates to observe the evolution of selected quantities at the vortex core or within the related vortex regions.

For a good overview of different vortex extraction methods, we refer to Fuchs et al. [FKS*10] and Post et al. [Pos03]. In addition, methods to analyze time-dependent

vector fields have been proposed; we refer to Pobitzer et al. [PPF*10] for an extensive overview of the recent publications. There are many promising approaches. For instance, several methods use the parallels vectors operator [PR00, FPH*08, WSTH07]. Others use topologically motivated algorithms to search for flow features [SVG*08].

In this paper, we make use of some widely used scalar quantities that indicate swirling flow behavior or vortices, respectively. Vorticity in two-dimensional flow fields is defined as the rate of rotation of a fluid particle. Its value is given by the difference of the non-diagonal entries of the Jacobian. Another quantity that is based on the Jacobian matrix is the Q-quantity as proposed by Hunt [Hun87]. For two-dimensional flow fields, the quantity was derived independently by Okubo [Oku70] and Weiss [Wei91]. Positive values of Q indicate that the vorticity tensor dominates the rate of strain tensor. Therefore, these regions are marked as vortices. Jeong and Hussain proposed the λ_2 value [JH95]. In their paper, they show that there is a correspondence between the Q-criterion and λ_2 for negative λ_2 values, which mark vortices. For two-dimensional fluid flows, these quantities can be easily converted into each other in these regions. Another criterion is based on the pressure field, for which the minima are often associated to vortex cores. For time-dependent flow fields, Haller [Hal01] proposed the finite-

time Lyapunov exponent (FTLE) to find structures of high separation or convergence. Recently, the acceleration magnitude was used to extract vortex cores in time-dependent flow fields. Kasten et al. [KHNH11] have shown that this quantity can be used as time-dependent counterparts of the critical points of standard vector field topology. Fuchs et al. [FKS*10] compared the minima to the FTLE, and the velocity magnitude. In their paper, they also proposed to use a measure called unsteadiness, the material derivative of the Jacobian of the velocity field. Recently, it was shown by Kasten et al. [KRHH11] that the region of influence of a vortex can be defined using the acceleration magnitude.

After the definition and extraction of vortex cores, the next step is to analyze these structures. A toolchain to analyze flow features was proposed by Reinders et al. [RPS01]. Stegmaier et al. [SRE05] proposed an exploration tool for vortical tools. After extracting vortices in a three-dimensional steady flow field based on the λ_2-criterion, they introduce a vortex browser to select and compare different kinds of vortices in a dataset. Schneider et al. [SWC*08] apply a contour tree extraction algorithm to different derived quantities such as λ_2 and pressure. They extract vortices as isosurfaces of these quantities. Their framework is able to find similarities between different features and it is applied to various three-dimensional steady flows. SimVis [DGH03] provides a software framework for the exploration of different feature definitions. One of the main applications is brushing the data and exploring the results in linked views. This concept is especially applicable to features lacking a concrete definition. Sahner et al. [SWTH07] used the Okubo-Weiss criterion to extract vortex and strain skeletons in three dimensional flows. Schafhitzel et al. [SBV*11] recently proposed a visualization and tracking system based on the λ_2 measure.

2. Foundation

The focus of this paper is to analyze and compare the evolution of vortex cores using different vortex definitions. Thereby, we restrict ourselves to methods that relate vortex cores to minima or maxima of a particular scalar quantity. The development of the vortex structures is then represented by the development of the extremal structure of the respective scalar field over time. For two-dimensional fields this results in an explicit one-dimensional structure given as a graph in three-dimensional space-time. Note that the physics of two-dimensional flows only allows vertex merges and no splits. Thus, this graph consists of multiple connected components, each representing one vortex merge tree.

The tracking of the extremal values is performed by tracing integral curves in a derived vector field in space-time, which is called feature flow field (FFF). Theisel et al. [TS03, WTvGP10] originally proposed this approach to track the critical points of vector field topology. It can easily be adapted to the context of scalar field topology to track ex-

tremal points of a scalar field. While this is an elegant way to describe the development of feature points, the method struggles in extracting stable structures in the presence of noise. Reininghaus et al. [RKWH12] proposed a combinatorial approach following a similar concept. It is designed to track critical points in scalar fields (extremal points and saddles) and is called combinatorial feature flow fields (CFFF). It makes use of homological persistence as proposed by Edelsbrunner [EHZ01] to treat noisy data. This enables a robust extraction of feature lines even in complex scalar fields. This method originally does not consider events like merges and splits of critical points. Due to its importance for flow analysis, Kasten at al. [KHNH12] put such events in the focus of their work. A variant of the CFFF approach, which is restricted to the pure tracking of extremal points, enables the extraction of vortex merge graphs in the combinatorial context. While Kasten et al. applied the extraction method to the acceleration magnitude, their approach is much more general. It can also be applied to other feature identifiers that indicate vortex cores as minima or maxima of the respective quantity. As this approach is the basis for our analysis, it is briefly summarized in the following.

2.1. Vortex merge graphs based on CFFF

The original approach is based on a combinatorial realization of a gradient vector field [RGH*10]. The advantage of this approach is the application of homological persistence [EHZ01] to simplify the combinatorial gradient field. This allows to remove spurious critical points from the topological skeleton, which makes the feature extraction robust against noise. For a time-dependent stack of combinatorial gradient fields, King [KKM08] introduced a tracking method that works directly on the simplified fields. Reininghaus et al. [RKWH12] has proposed an efficient computation of this tracking approach. For the case of minima or maxima, the basic idea of CFFF can be summarized as follows: Two minima or maxima of adjacent time slices are connected, if they fall in the topological basin of each other.

The approach defines two different functions: a forward tracking $F_t : C_t \rightarrow C_{t+1}$ and a backward tracking $B_t : C_t \rightarrow C_{t-1}$. They assign a critical point $c_1 \in C_t$ to another critical point c_2 in the next or previous time step, respectively, if c_1 falls into the basin of c_2. Two critical points c_1, c_2 of subsequent time steps are called *uniquely* tracked, if $F_t(c_1) = c_2$ and $B_{t+1}(c_2) = c_1$. Let M be the set of all uniquely tracked lines. Now, Kasten et al. [KHNH12] extended this approach by defining connections between these lines to extract mergers of vortex cores. The following condition is tested for each end point of a line $e_t \in M$: $\exists T > 0 : F_{t+T}(...F_{t+1}(F_t(e_t))) \in M$. Loosely speaking, it is tested if the repeated evaluation of the forward tracking of the end point hits another tracked core line. If such a T is found, the line given by $F_{t+T}(...F_{t+1}(F_t(e_t)))$ is added to the result. This results in a vortex merge graph.
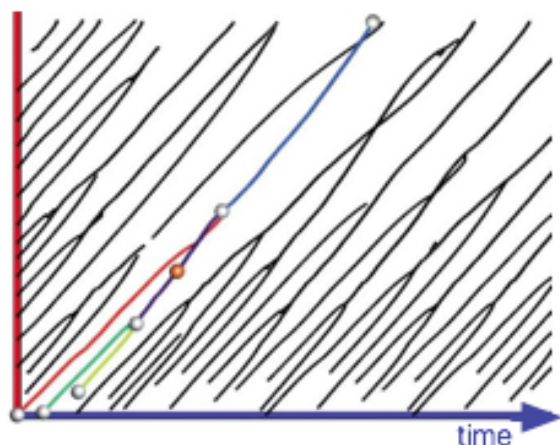
Figure 1: *Picking and segmentation of a singel vortex merge tree. The spheres highlight the merge events for the selected tree.*

(a) λ_2

(b) Vorticity

(c) Acceleration magnitude

Figure 2: *Segmentation of vortex merge graphs for three different scalar identifiers, as used in Fig. 3*

3. Explorative Tools

The various definitions of vortex cores reflect different views onto the topic of vortex analysis and coherent structure in flow fields. Each definition focusses on different physical properties. To understand how theses quantities are related and which quantity is more appropriate in which context motivates a thorough analysis of the resulting structures. Differences and similarities of the structures themselves, and also the values of other quantities along the structures are of high interest. The availability of explicit merge graphs for different measures provides a good basis for such an analysis. The following analysis considers scalar feature identifiers along extracted core lines and for vortex regions as defined in [KRHH11].

3.1. Analysis of Vortex Core lines

The analysis of the vortex core lines consists of two components: First, from the complete merge graph subsets consisting of single trees can be interactively selected and highlighted for further inspection. This allows to focus on single vortices and their evolution. Second, different quantities sampled along this tree can be statistically analyzed and visualized. The approach supports common concepts as brush-and-link, scatter plots and parallel coordinates.

Selection – For the comparison of vortex merge graphs, which result from different scalar identifiers, it is necessary to be able to concentrate on selected vortices and their development in time. Therefore our system supports an interactive selection of vortex structures by picking a point on the vortex merge tree. All substructures that belong to the selected tree are then extracted from the graph and segmented into individual vortices, see Fig. 1. The subgraph is therefore split into segments that contain no merge event. These
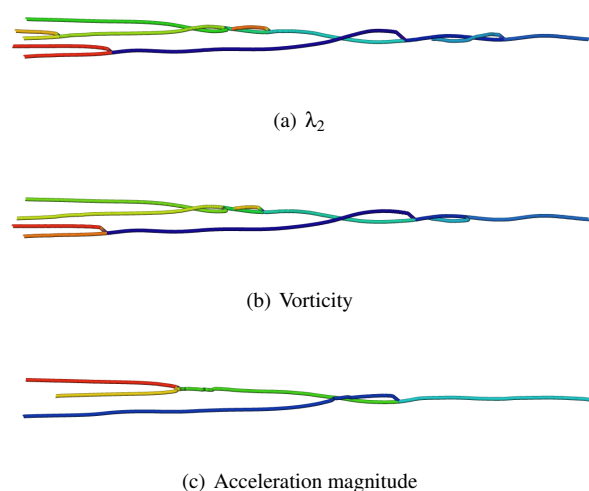

(a) λ_2
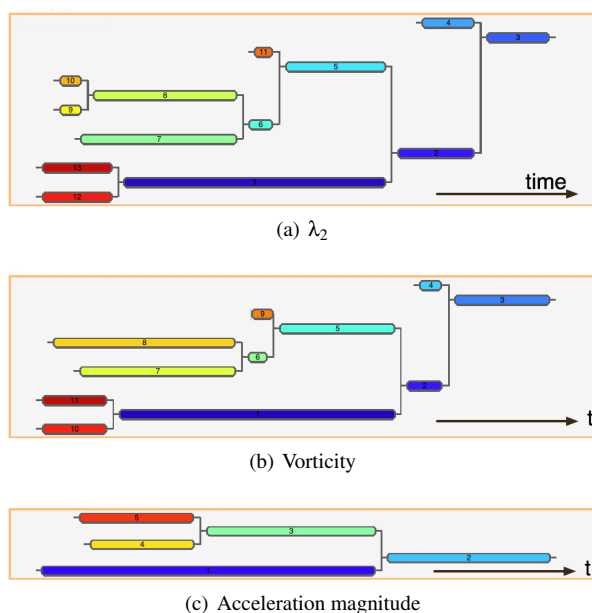
(b) Vorticity

(c) Acceleration magnitude

Figure 3: *Abstract vortex merge graphs extracted using three different quantities: vorticity, λ_2, and the acceleration magnitude. The original merge graphs are shown in Fig. 2*

individual vortices are then used to define a representation that abstracts from the spatial embedding of the vortex tree highlighting the temporal development. These vortices are assigned an iconic representation expressing their lifetime. The exact times of birth, death or merge of these vortices determine their placement on the time-line. Merge events are shown by lines connecting the single vortices. This ab-

stract representation of the tree facilitates an easy comparison of vortex graphs based on different feature identifiers, see Fig. 3. A color coding provides the necessary reference to the spatial representation. On basis of this representation parts of the merge tree can be switched off and on for the statistical analysis. For each selected substructure, the visualization tools described below can be applied.

Visualization – Monitoring essential quantities along the selected structures is a first step in evaluating the extracted structures. While the merge tree displays the center of the vortex, the corresponding scalar values give a hint about its strength. Selected quantities can be displayed along the abstract graph as function plots, Fig. 7.

Parallel coordinates provide a first insight into the correlation of different scalar measures of interest. The quantities are sampled along the merge graph. Due to the high temporal resolution it suffices to display the information for every *n*-th point on the graph. This reduces visual clutter and removes redundant information. To provide a better visual perception, areas of high line density are darkened by rendering the lines of the parallel coordinates as *glow lines*. This is done by rendering each line l_i as a stripe with width d and decaying opacity from the centerline to its boundary in a subtractive color model. In detail, let p be the current pixel, $O_{l_i,p}$ be the opacity of line l_i at pixel p, $C_{l_i,p}$ be the color of line l_i at pixel p, and C_B be the background color, which is white in our case. The color C_p of pixel p is then:

$$C_p = C_B - \sum_{i=1}^{N} C_{l_i,p} \cdot O_{l_i,p}$$

Note that only lines with a maximum distance d to p have to be considered. The rendering of the glow lines as stripes is done using the approach of Merhof et al. [MSE*06]. The use of glow lines results in smooth parallel coordinates by composing the individual lines. An example is depicted in Fig. 4.

The second exploration technique reveals correlations between quantities by use of scatter plots. In both of these plots, the user can select interesting structures. The selection is then highlighted in the spatial representation of the graph.

3.2. Analysis of Vortex Vicinity

To analyze the vicinity of a vortex, we consider two different options. The first option includes a circular region, with a user defined radius around the vortex core, into the analysis. The second option is more physically based and related to the acceleration magnitude. Vortex-like minima of the acceleration magnitude are enclosed by particularly pronounced ridges providing a natural vortex region definition [KRHH11]. For both options we provide the following analysis tools: First, the different flow quantities are visualized on the respective area as color map. This gives the user
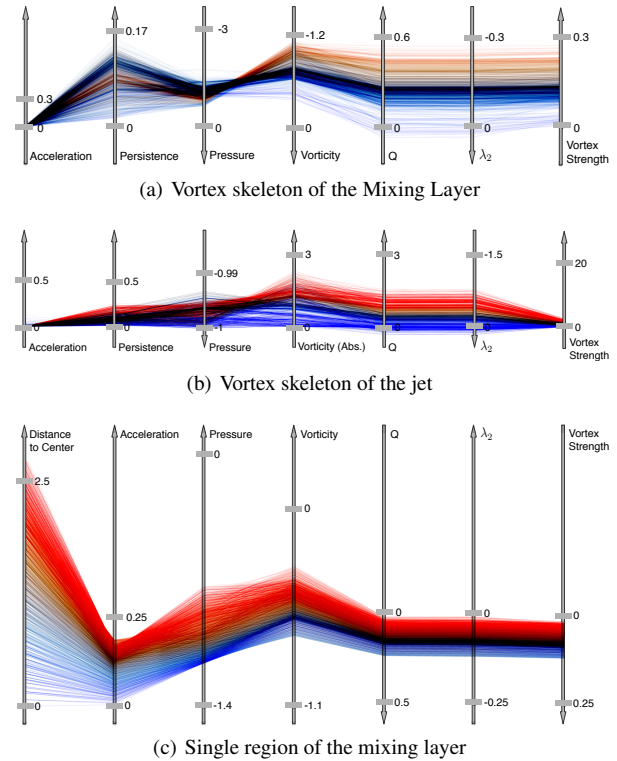

(a) Vortex skeleton of the Mixing Layer

(b) Vortex skeleton of the jet

(c) Single region of the mixing layer

Figure 4: *Parallel coordinate plot of a set of sample points on the vortex skeleton of the mixing layer (a), and the jet (b), and a single representative region of the mixing layer (c). The color of the lines is chosen by the vortex strength measure (a,b), or the distance to the vortex core the region is associated to (c). For a better visual perception the quantities are scaled, shifted and mirrored – as indicated by the gray bars. For all plots, vorticity, λ_2, Q and the vortex strength measure show very similar behavior and, thus, contain redundant information.*

a first impression of their behavior. To indicate their correlation along the vortex regions, we make use of the parallel coordinates and scatter plots mentioned above. It is thereby possible to represent the quantities for a set of regions sampled along the selected graph or one individual region.

To get an idea of the distribution of the scalar values inside the regions along a selected subgraph a further statistical analysis is of interest. For this purpose a more complex tool is provided. Its interface, depicted in Fig. 9, consists of three parts: At the top, an abstract representation of the vortex graph is given. Time is thereby represented by the *x*-direction. Each segment of the vortex merge graph is a toggle to select this structure in the plots. An optional coloring of the buttons links the segments to their spatial representation and the corresponding plots. In the second part, different plots of the quantities can be shown. Again, the *x*-axis
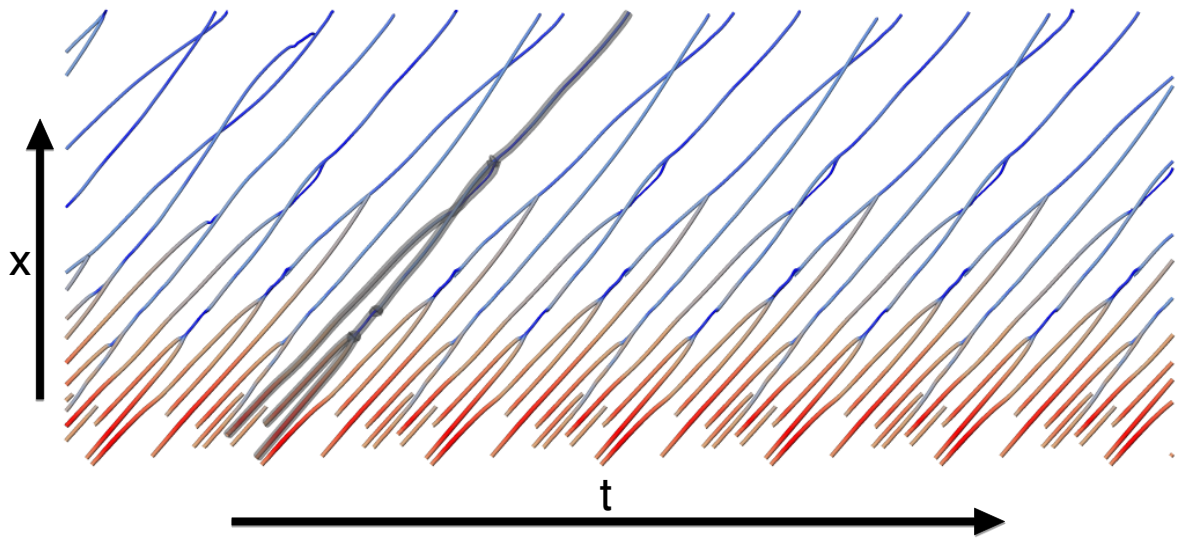
Figure 5: *Vortex merge graph of the mixing layer dataset extracted from the acceleration magnitude. The time goes from left to right and the flow from bottom to top. Both, radius and color of the depicted vortex cores depend on the vorticity magnitude: low and high vorticity correspond to blue/thin and red/thick, respectively.*

represents the time and the *y*-axis the values of the selected quantity. Mean, median, minimum and maximum values and percentiles are visualized by lines and box plots. The third part of the user interface optionally shows the area of the associated vortex region. This helps to identify correspondence between the development of a quantity and the size of the vortex region. Again, depending on the related questions, statistical values can be displayed as individual curves for each segment or as integral value. This is especially interesting when asking questions related to the conservation of certain entities, e.g. vorticity.

4. Results

The data set that is considered for our analysis is a two-dimensional mixing layer. It represents a shear flow with a velocity ratio between upper and lower stream of 3:1 [CSB98, NPT*04, NPM05]. The inflow is described by a tanh profile with a stochastic perturbation. The Reynolds number based on maximum velocity and vorticity thickness is 500. The flow is computed with a compact finite-difference scheme of 6th order accuracy in space and 3rd oder accuracy in time. The computational domain $(x, y) \in [0, 140] \times [-28, 28]$ is discretized on a 960×384 grid. The sampling time for the employed snapshots is $\Delta t = 0.05$ corresponding 1/10 of the computational time step.

We use a second data set to validate our results: a jet. It is also a two-dimensional time-dependent flow and shows a number of vortex mergers. The convection velocity of these

vortices is not constant but decreases in stream-wise direction.

The starting point of our analysis is the extraction of the vortex merge graph as shown in Fig. 5. It was extracted using the acceleration magnitude. In this figure, a selected subgraph is depicted that serves as a reference for the further analysis.

In Fig. 2 (c), this subgraph and its segmentation is shown. At the same point in the data set, we also computed vortex merge graphs based on vorticity and λ_2 as shown in Fig. 2 (a+b). They represent the same vortices in the flow, but are now identified by different quantities. Note that we removed short-living vortex cores from the vortex merge graphs resulting from vorticity and λ_2. In Fig. 3, the abstract representations of these subgraphs are shown. Obviously, vorticity and λ_2 yield more complex vortex merge structures than the acceleration magnitude. We can also see that for vorticity and λ_2, there are more vortices connected to the graph at the beginning. Note that these vortices are visible in the acceleration magnitude, but not connected to the merge graph. This was already observed by Kasten et al. [KHNH12].

To investigate the behavior of flow quantities along the merge graph, these quantities are sampled along the complete vortex skeleton and plotted as parallel coordinates in Fig. 4 (a). The coloring of the lines is determined by the vortex strength measure. The coordinate axes were scaled to provide a good visual perception of the correspondences. The acceleration magnitude is zero along the vor-
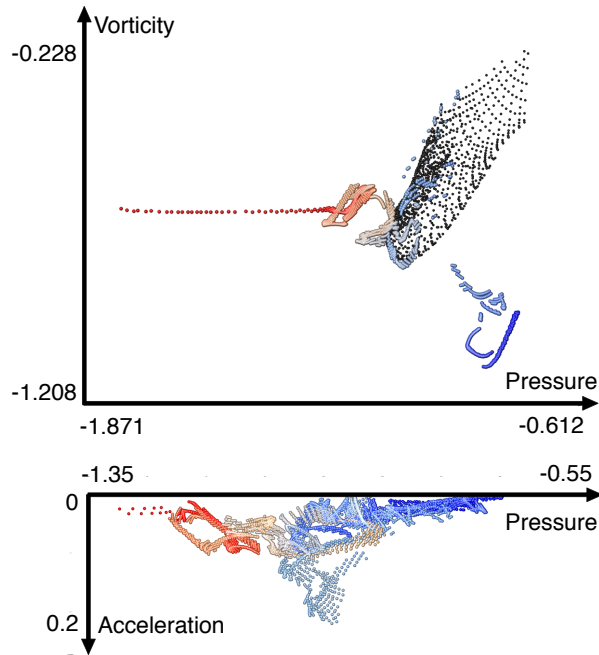
Figure 6: *Scatter plot of the pressure compared to the vorticity (top) and the acceleration (bottom) sampled along the vortex merge graph extracted from the acceleration magnitude (top) and the vorticity (bottom). The coloring indicates time – blue corresponds to earlier and red to later times.*

Figure 7: *Scatter plot of the mean of the vorticity in a vortex region compared to its size. The measures are sampled along the merge graph identified by the acceleration magnitude. The coloring indicates the time – blue corresponds to earlier and red to later times.*

tex core lines. As expected, vorticity, Q, λ_2, and the vortex strength measure exhibit very similar behavior on the lines. In Fig. 4 (b), we validated this correspondence with the data set of a jet. Due to the strong correlation of theses quantities, we restrict the further analysis to vorticity, pressure, λ_2 and the acceleration magnitude.

To compare the vorticity with the acceleration magnitude, we plotted the different quantities along the selected vortex cores of Fig. 2 as scatter plots against the pressure in Fig. 6. The coloring of the points is determined by the time. To the top image, we added a scatter plot of the same quantities on a vortex region in the middle of the graph. While in both images the pressure decreases with time, the other quantities show different behavior. In the top image, the vorticity increases with time and is nearly constant after the last vortex merge. This could be related to vorticity transport as discussed by Sadlo et al. [SPS06]. During the merge events, there is a chaotic behavior of the vorticity. The black dots indicating the behavior on a representative vortex region reveal that the vorticity and the pressure are significantly higher within the region than at the vortex core. Note that vorticity is negative here.

As a next step, we analyzed the behavior of vorticity in the vortex region. We plotted the mean value of the vorticity
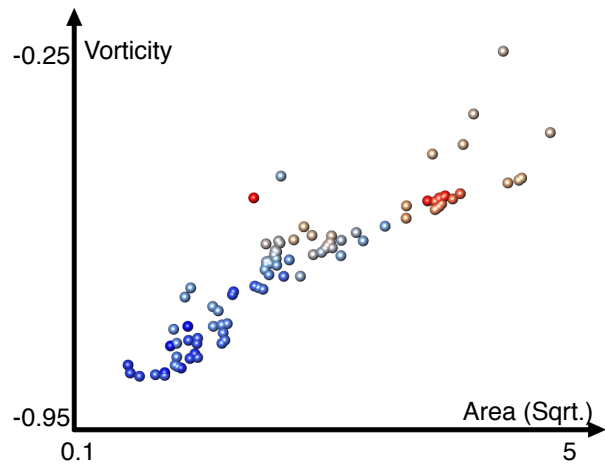
against the square root of the area of the associated vortex region along the vortex merge graph identified by the acceleration magnitude as selected in Fig. 2 (c). The resulting scatter plot, see Fig. 7, suggests a linear correspondence between these measures.

Finally, we used our analysis tools with the two selected merge graphs. Fig. 8 shows the plot of a sampling of the acceleration magnitude on a circular disk along the vorticity graph. We removed the L-shaped short-living vortex cores from the vorticity graph depicted in Fig. 2 for these images to focus on the main merge structures. Fig. 9 shows the plot of the sampling of the vorticity on the vortex regions along the acceleration graph. At the top the abstract graph is represented. The user can select different subgraphs. In the middle, the options for the plot are shown. For the two images, we chose to show the coloring of the abstract graph and the box plots. At the bottom, the box plots show the distribution of the vorticity or acceleration, respectively, along the graph. The centerline corresponds to the mean value of the particular quantity. Along the vorticity merge graph, the mean of the acceleration constantly grows, but stays nearly constant after the last merge. The minimum value is always zero. For the vortex merge graph resulting from the acceleration magnitude, we added the minimum line of the vorticity and the area of the vortex region in an extra plot. Outside the influence of a vortex merge, the mean of the vorticity and the area of the vortex region stay relatively constant along the acceleration graph. The minimal values of the vorticity increase a bit. Within the merge window, both the mean of the vorticity and the area increase drastically. As suggested by the literature, the vorticity should stay constant in a vortex
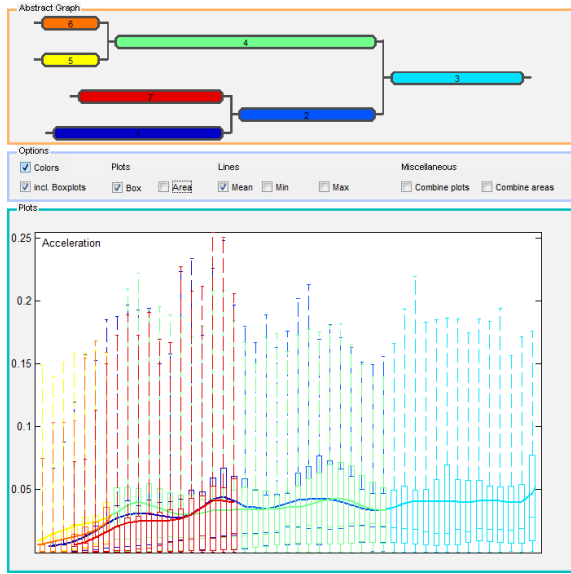
Figure 8: *Analysis of the vortex merge graph indicated by the vorticity. The acceleration magnitude in a circular region of size 17 is sampled along the graph and indicated by box plots at the bottom. In addition, the mean value of the acceleration is shown as a thick line. The coloring at the bottom corresponds to the color of the segments of the merge graph at the top.*
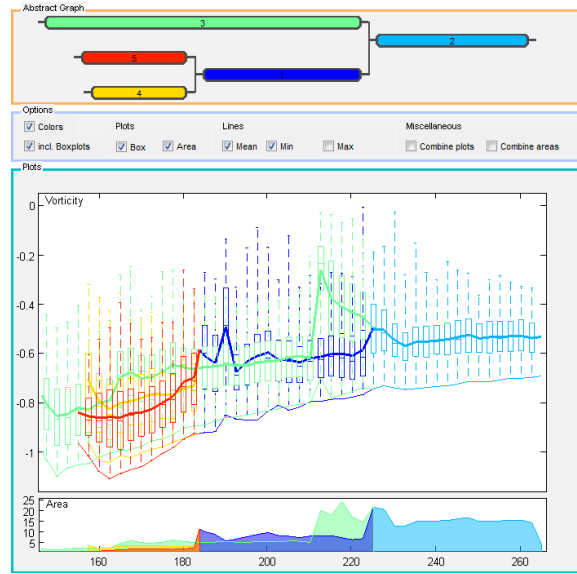

Figure 9: *Analysis of the vortex merge graph indicated by the acceleration magnitude. The vorticity is sampled in the vortex regions along the graph and indicated by box plots in the center. In addition, the mean value of the voriticity is shown as a thick line. The coloring at the bottom corresponds to the color of the segments of the merge graph at the top. The area of the vortex regions is plotted at the bottom.*

region. This is partially validated outside the vortex merge windows.

5. Conclusion

In this paper, we investigated the vortex merge graphs extracted from the acceleration magnitude, vorticity and λ_2. We proposed an analysis framework to get insight into the merge behavior and the correspondence of different flow quantities to each other. This includes a tool that provides a simple user interface to select parts of the explicitly extracted vortex merge graphs and visualize quantities along these graphs and their regions of influence using statistical utilities. We prove the usability of our framework by applying them to a DNS simulated data set of a mixing layer

The utilization of scatter plots and parallel coordinates allowed us to investigate the vortex merge graphs as proposed by Kasten et al. [KHNH12]. The explicit representation of vortex merge structures enable the sampling of different flow quantities along vortex core lines. This helps the users to better understand the vortices itself and the differences between the observables used to extract the core lines. We were also able to verify the correspondence of flow quantities using the parallel coordinates plots.

The recently proposed definition of vortex regions based

on the acceleration magnitude is parameter independent and physically well motivated. In this paper, we used it to analyze different flow quantities not only along vortex cores but also within their region of influence. The proposed tool presents the user selected subgraphs of the vortex merge graphs in an abstract way. By selecting particular vortex core lines, a plotting area shows the minimum, maximum, median, mean and other percentiles of quantities sampled in these vortex regions. The user can therefore get insight into the behavior of flow quantities, which hopefully enables a better understanding. Currently, there is no unique definition of a vortex. Our tools provide multiple viewpoints onto flow behavior in a general fashion. They are not restricted to a special quantity such as the acceleration, but work with arbitrary measures such as vorticity, pressure or λ_2.

Acknowledgments

References

[CSB98] COMTE P., SILVESTRINI J. H., BÉGOU P.: Streamwise vortices in large eddy simulations of mixing layer. *European Journal of Mechanics B 17* (1998), 615–637. 5

[DGH03] DOLEISCH H., GASSER M., HAUSER H.: Interactive feature specification for focus+context visualization of complex simulation data. In *Proceedings Joint EG - IEEE TVCG Symposium on Visualization 2003* (2003), pp. 239–248. 2

[EHZ01] EDELSBRUNNER H., HARER J., ZOMORODIAN A.: Hierarchical morse complexes for piecewise linear 2-manifolds. In *Proceedings Symposium on Computational Geometry 2001* (2001), pp. 70–79. 2

[FKS*10] FUCHS R., KEMMLER J., SCHINDLER B., WASER J., SADLO F., HAUSER H., PEIKERT R.: Toward a Lagrangian vector field topology. *Computer Graphics Forum 29*, 3 (2010), 1163–1172. 1, 2

[FPH*08] FUCHS R., PEIKERT R., HAUSER H., SADLO F., MUIGG P.: Parallel vectors criteria for unsteady flow vortices. *IEEE Transactions on Visualization and Computer Graphics 14*, 3 (2008), 615–626. 1

[Hal01] HALLER G.: Distinguished material surfaces and coherent structures in three-dimensional fluid flows. *Physica D 149* (2001), 248–277. 1

[Hun87] HUNT J. C. R.: Vorticity and vortex dynamics in complex turbulent flows. *Transactions of the Canadian Society of Mechnical Engineering 11* (1987), 21–35. 1

[JH95] JEONG J., HUSSAIN A. K. M. F.: On the identification of a vortex. *Journal of Fluid Mechanics 285* (1995), 69–94. 1

[KHNH11] KASTEN J., HOTZ I., NOACK B., HEGE H.-C.: On the extraction of long-living features in unsteady fluid flows. In *Topological Methods in Data Analysis and Visualization* (2011), Springer, pp. 115–126. 2

[KHNH12] KASTEN J., HOTZ I., NOACK B., HEGE H.-C.: Vortex merge graphs in two-dimensional unsteady flow fields. In *Proceedings Joint EG - IEEE TCVG Symposium on Visualization 2012 – Short Paper* (2012). 1, 2, 5, 7

[KKM08] KING H., KNUDSON K., MRAMOR N.: Birth and death in discrete morse theoryorse theory. *arXiv:0808.0051v1* (2008). 2

[KRHH11] KASTEN J., REININGHAUS J., HOTZ I., HEGE H.-C.: Two-dimensional time-dependent vortex regions based on the acceleration magnitude. *IEEE Transactions on Visualization and Computer Graphics 17* (2011), 2080–2087. 2, 3, 4

[MSE*06] MERHOF D., SONNTAG M., ENDERS F., NIMSKY C., HASTREITER P., GREINER G.: Hybrid visualization for white matter tracts using triangle strips and point sprites. *IEEE Transactions on Visualization and Computer Graphics 12* (2006), 1181–1188. 4

[NPM05] NOACK B. R., PAPAS P., MONKEWITZ P. A.: The need for a pressure-term representation in empirical Galerkin models of incompressible shear flows. *Journal of Fluid Mechanics 523* (2005), 339–365. 5

[NPT*04] NOACK B. R., PELIVAN I., TADMOR G., MORZYŃSKI M., COMTE P.: Robust low-dimensional Galerkin models of natural and actuated flows. In *Proceedings Fourth Aeroacoustics Workshop 2004* (2004). 5

[Oku70] OKUBO A.: Horizontal dispersion of floatable particles in the vicinity of velocity singularities such as convergences. *Deep Sea Research and Oceanographic Abstracts 17*, 3 (1970), 445 – 454. 1

[Pos03] POST F. H.: The state of the art in flow visualization: Feature extraction and tracking. *Computer Graphics Forum 22*, 4 (2003), 775–792. 1

[PPF*10] POBITZER A., PEIKERT R., FUCHS R., SCHINDLER B., KUHN A., THEISEL H., MATKOVIC K., HAUSER H.: On the way towards topology-based visualization of unsteady flow - the state of the art. In *Proceedings Eurographics 2010* (2010), pp. 137–154. 1

[PR00] PEIKERT R., ROTH M.: The parallel vectors operator - a vector field visualization primitive. In *Proceedings IEEE Visualization 2000* (2000), pp. 263–270. 1

[RGH*10] REININGHAUS J., GÜNTHER D., HOTZ I., PROHASKA S., HEGE H.-C.: TADD: A computational framework for data analysis using discrete Morse theory. In *Proceedings International Congress on Mathematical Software 2010* (2010), pp. 198–208. 2

[RKWH12] REININGHAUS J., KASTEN J., WEINKAUF T., HOTZ I.: Efficient computation of combinatorial feature flow fields. *IEEE Transactions on Visualization and Computer Graphics – in press 99* (2012). 2

[RPS01] REINDERS F., POST F. H., SPOELDER H. J. W.: Visualization of time-dependent data using feature tracking and event detection. *The Visual Computer 17*, 1 (2001), 55–71. 2

[SBV*11] SCHAFHITZEL T., BAYSAL K., VAARANIEMI M., RIST U., WEISKOPF D.: Visualizing the evolution and interaction of vortices and shear layers in time-dependent 3D flow. *IEEE Transactions on Visualization and Computer Graphics 17*, 4 (2011), 412–425. 2

[SPS06] SADLO F., PEIKERT R., SICK M.: Visualization tools for vorticity transport analysis in incompressible flow. *IEEE Transactions on Visualization and Computer Graphics 12*, 5 (2006), 949–956. 6

[SRE05] STEGMAIER S., RIST U., ERTL T.: Opening the can of worms: An exploration tool for vortical flows. In *Proceedings IEEE Visualization 2005* (2005), pp. 463–470. 2

[SVG*08] SCHAFHITZEL T., VOLLRATH J. E., GOIS J. P., WEISKOPF D., CASTELO A., ERTL T.: Topology-preserving lambda$_2$-based vortex core line detection for flow visualization. *Compututer Graphics Forum 27*, 3 (2008), 1023–1030. 1

[SWC*08] SCHNEIDER D., WIEBEL A., CARR H., HLAWITSCHKA M., SCHEUERMANN G.: Interactive comparison of scalar fields based on largest contours with applications to flow visualization. *IEEE Transactions on Visualization and Computer Graphics 14*, 6 (2008), 1475–1482. 2

[SWTH07] SAHNER J., WEINKAUF T., TEUBER N., HEGE H.-C.: Vortex and strain skeletons in eulerian and Lagrangian frames. *IEEE Transactions on Visualization and Computer Graphics 13*, 5 (2007), 980–990. 2

[TS03] THEISEL H., SEIDEL H.-P.: Feature flow fields. In *Proceedings Joint EG - IEEE TCVG Symposium on Visualization 2003* (2003), pp. 141–148. 2

[Wei91] WEISS J.: The dynamics of enstrophy transfer in two-dimensional hydrodynamics. *Physica D: Nonlinear Phenomena 48* (1991), 273–294. 1

[WSTH07] WEINKAUF T., SAHNER J., THEISEL H., HEGE H.-C.: Cores of swirling particle motion in unsteady flows. *IEEE Transactions on Visualization and Computer Graphics 13*, 6 (2007), 1759–1766. 1

[WTvGP10] WEINKAUF T., THEISEL H., VAN GELDER A., PANG A.: Stable feature flow fields. *IEEE Transactions on Visualization and Computer Graphics 17*, 6 (2010), 770–780. 2